Available online at www.sciencedirect.com
SCIENCE DIRECT®
Pergamon
Cement and Concrete Research 33 (2003) 1681–1686
CEMENT AND CONCRETE RESEARCH

Uptake and loss of water in a cenosphere–concrete composite material

Nikhil Barbare[a], Arun Shukla[b], Arijit Bose[a,*]

[a]Department of Chemical Engineering, University of Rhode Island, Kingston, RI 02881, USA
[b]Department of Mechanical Engineering, University of Rhode Island, Kingston, RI 02881, USA

Received 1 May 2002; accepted 14 April 2003

Abstract

Cenospheres are hollow, aluminum silicate spheres, between 10 and 300 μm in diameter. Their low specific gravity (0.67) makes them ideal replacements for fine sand for producing low-density concrete. In an effort to understand the potential for practical use of the cenospheres as a fine aggregate in concrete, the moisture uptake and loss by cenospheres and water uptake and loss in cenosphere–concrete composites have been studied in this paper. The equilibrium moisture content of cenospheres is about 18 times higher than that of sand, reflecting the porous nature of cenospheres. The temporal evolution of water penetration into the cenosphere–concrete is modeled using Washburn kinetics. The effective pore size using this model is of the order of several nanometers. These results imply a lack of connectivity within the pores, leading to a low permeability. SEM images of the concrete reveal pore sizes of the order of 2–5 μm. The drying flux for cenospheres shows a classical behavior—a constant rate followed by a linear falling rate period. Thus, experiments done at these conditions can be used to predict drying times for wet cenospheres exposed to other environments. The flux of water vapor away from both the cenosphere–concrete as well as the normal concrete shows a nonlinear change with moisture content throughout the drying cycle, implying that the pore structure within the concrete strongly influences the drying behavior.

Keywords: Humidity; Drying; Microstructure; Permeability; Cenospheres

1. Introduction

Cenospheres are hollow aluminum silicate microspheres obtained from the fly ash of coal-fired thermal power plants. Their diameters vary from 10 to 300 μm, with a typical wall thickness of about 5–10% of the diameter. Fig. 1a and b show SEM images of cenospheres, clearly showing their size, hollow nature, and their porosity. They have a specific gravity of 0.67 and a bulk density of 375 kg/m^3. Their chemical composition is primarily silica (65%) and alumina (30%) with trace amount of oxides of Fe, Ca, K, and Ti. As a constituent in composite materials, these cenospheres have enormous potential to reduce density, provide better insulation, improve impact resistance, and reduce shrinkage and warpage [1–3]. Coal-fired power plants produce abundant quantities of these spheres (as high as 40 million tons per plant per year), which are normally disposed of in landfills. Their spherical and hollow morphology, chemical characteristics, as well as their mechanical and energy-attenuating properties can be exploited synergistically with those of cement to form lightweight materials suitable for bridge decks, pavements, and highways. The main advantage presented by cenospheres in comparison with other competitive filling compounds is their low density [4–6].

The water content in concrete has a significant impact on its mechanical properties. Moisture transport in porous media plays an important role in the degradation of building materials such as mortar and concrete [7]. When cenospheres are used to replace the fine aggregates in concrete, the inherent differences in the equilibrium moisture content require different amounts of water to be added prior to curing the concrete. In the first set of experiments reported here, the equilibrium moisture content, as well as the kinetics of water vapor uptake of cenospheres, is compared to fine sand. Thus, these experiments provide a useful metric for sample preparation, since they quantify the amount of water bound to the cenospheres and therefore not available for the cement.

* Corresponding author. Tel.: +1-401-874-2804; fax: +1-401-874-4689.
E-mail address: bosea@egr.uri.edu (A. Bose).

0008-8846/03/$ – see front matter © 2003 Published by Elsevier Ltd.
doi:10.1016/S0008-8846(03)00148-0

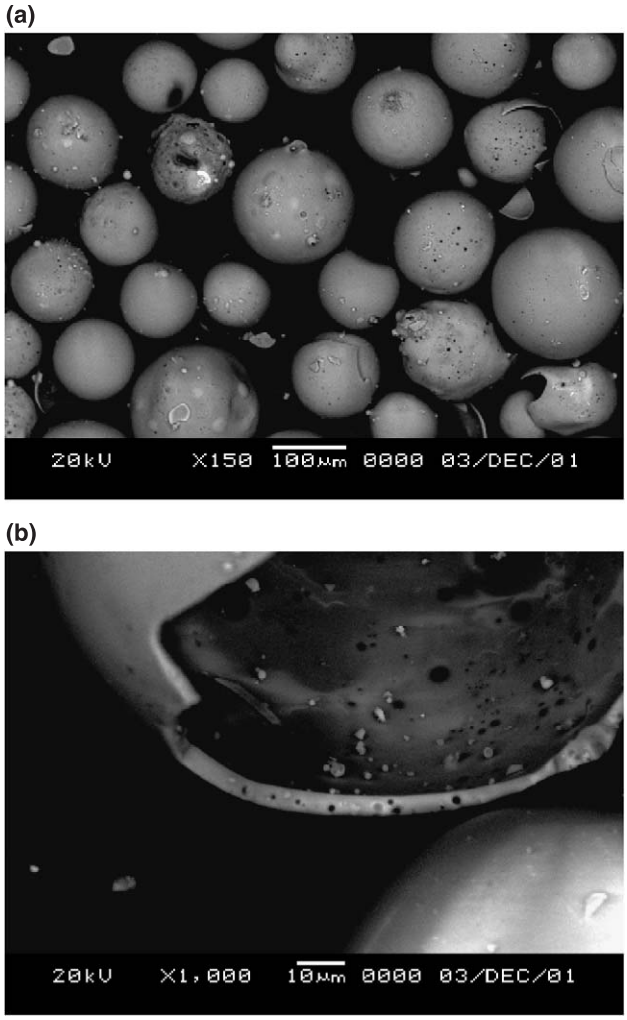

Fig. 1. (a) SEM micrograph of the cenospheres indicating the porous inner/outer surfaces. (b) A section of porous and thin walls of a broken cenosphere.

An important factor that impacts the durability of concrete is the uptake and loss of water. Ingress of water in the concrete provides a path for the transport of deleterious materials such as chloride and sulfate ions. This leads to corrosion of reinforcement bars and substantial deterioration in the mechanical properties and service life of the concrete. Corrosion leads to loss of steel–concrete bond with detrimental consequences on the load-carrying capacity of structure [8]. The penetration of water into the pores in concrete can also lead to undesirable cracking during freezing [9]. The second set of experiments is geared towards monitoring and comparing water penetration in cenosphere–concrete and normal concrete.

Concrete used in structural applications is often exposed to environments that can be extremely dry. Under those conditions, it is important to understand the rate of loss of water. In the third set of experiments, moisture loss in cenosphere–concrete composites as well as normal concrete are monitored at 23, 30, and 40 °C using air of 45% relative humidity.

2. Materials and methods

2.1. Moisture uptake

Cenospheres and fine sand (Grading 1, ASTM C-637) samples weighing 1.63 and 3.50 g (each sample had the same volume), respectively, were exposed to a constant temperature (23 °C) and constant relative humidity (85%) environment inside a closed chamber. The moisture uptake in the samples was monitored over time by measuring the mass of the samples at regular intervals. A plot of the fractional weight gain (weight of water absorbed/dry weight of sample) over time for the cenospheres and sand is shown in Fig. 2.

The equilibrium moisture content of cenospheres exposed to air of 85% relative humidity is 0.15 kg water/kg dry cenospheres. For sand, this number is 0.0084 kg water/kg dry solid. This 18-fold difference in the moisture absorption capacity is caused by the porous nature of cenospheres.

2.2. Preparation of cenosphere–concrete sample for water influx and drying

The concrete test specimen was prepared according to the ASTM standard C 192. The cenosphere–concrete is formed by replacing all the fine sand in the normal concrete by cenospheres. The volume percent of cenospheres in the composite sample is 30%. The density of the normal concrete is 2307 kg/m^3, while that of the cenosphere–concrete is 2000 kg/m^3. The specimens were disks of diameter 0.1 m and thickness 0.022 m. The disks were sliced from a cast cylindrical specimen of dimensions 0.1 m diameter and 0.2 m height. They were dried at 50 °C to achieve a constant weight and then exposed to water in a bath as shown in Fig. 3. Covering the surface tightly with an impermeable plastic sheet eliminated water penetration from the curved surface. The mass of the specimen was measured using an electronic balance (with a resolution of 1 g) at

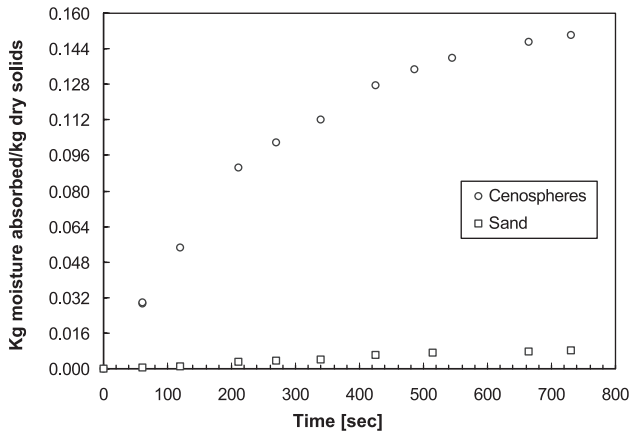

Fig. 2. Fractional weight gain versus time for the cenospheres and sand. The equilibrium moisture content of cenospheres is large compared to that in sand.

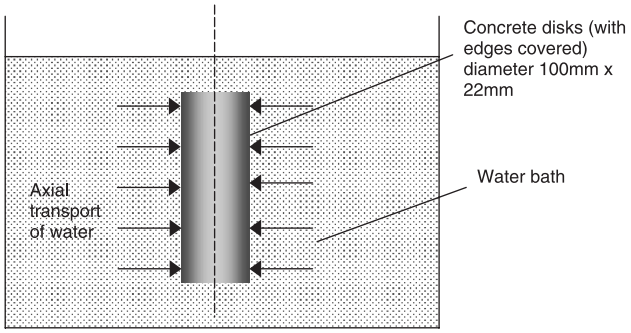

Fig. 3. Schematic of the experimental setup for penetration of water in the concrete. Axial transport of water in the concrete from both the flat surfaces.

regular intervals. The weight gain by the specimens is calculated and is normalized by the initial dry weight of the sample.

2.3. Absorption of water

The normalized weight gain in the concrete samples is plotted versus time in Fig. 4. Note that water uptake in both the samples is extremely slow, showing saturation after approximately 4 days. Over the first 2 h, the water absorption profiles for the normal and cenosphere–concrete are very similar when seen at this scale. However, the equilibrium moisture content for the lightweight concrete is 1.16×10^{-2} kg water/kg dry concrete, more than the equilibrium moisture content of 9.425×10^{-3} kg water/kg dry concrete for the normal concrete. The material properties of concrete depend on the mix design, preparation, and environmental conditions [9]. Thus, the concrete properties can be somewhat variable. However, because the only change in the sample preparation is the replacement of fine sand with cenospheres, these data are a useful comparison between the two types of concrete.

Since the water penetration is driven by capillary transport in a porous medium like concrete, this process is modeled using Washburn kinetics [10].

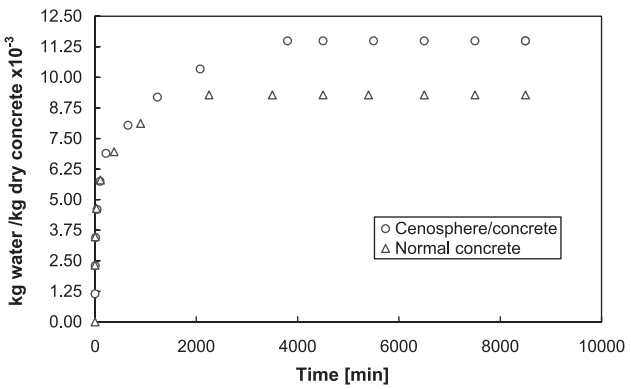

Fig. 4. Fractional weight gain versus time for the cenosphere–concrete and normal concrete samples. Absorption of water by cenosphere–concrete is more than normal concrete.

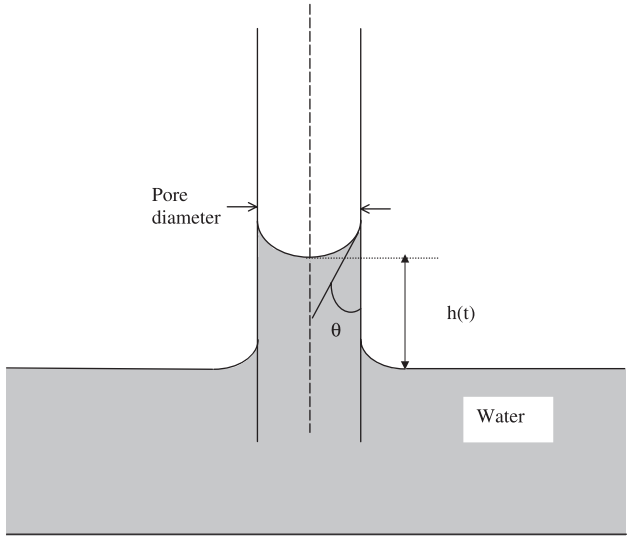

Fig. 5. Forces acting on water transport due to capillary rise in concrete pore. A contact angle θ is obtained where the fluid–fluid interface meets a solid surface.

Neglecting inertia, the instantaneous force balance on a slug of liquid rising in a cylindrical pore is (see Fig. 5)

$$2\pi r_c \gamma \cos\theta - 2\pi r_c \tau h(t) = 0 \quad (1)$$

Here r_c is the effective pore radius, γ is the surface tension of water (72×10^{-3} N/m at 23 °C), θ is the wetting angle, τ is the viscous shear stress acting on the fluid at the wall, and $h(t)$ is the liquid penetration depth at time t. The first term represents the capillary force, while the second term is the viscous drag (since the experiments were performed with water absorption from the lateral faces of the sample; effects of gravity are neglected).

Assuming that the flow in the pore is fully developed, the viscous shear stress, τ, for a Newtonian liquid is given by:

$$\tau = \frac{4\mu}{r_c}\bar{V} = \frac{4\mu}{r_c}\frac{dh}{dt} \quad (2)$$

where, $\bar{V}$ is the mean velocity of liquid, $\bar{V} = dh/dt$

Substituting Eq. (2) into Eq. (1),

$$2\pi r_c \gamma \cos\theta - 2\pi r_c \left(\frac{4\mu}{r_c}\frac{dh}{dt}\right) h$$

which can be rearranged to give

$$h\frac{dh}{dt} = \frac{r_c \gamma \cos\theta}{4\mu} \quad (3)$$

Integrating Eq. (3) and using the condition that $h(0) = 0$ gives

$$h(t) = \sqrt{\frac{r_c \gamma \cos\theta}{2\mu} t} \quad (4)$$

The penetration depth $h(t)$ is obtained from the experimental measurement of weight gain $\Delta W(t)$ from

$$\Delta W(t) = 2h(t)A\rho\varepsilon \tag{5}$$

Here, A is the area of cross section, ρ is density of water, and ε is the porosity of the concrete. ε is calculated using the data for the actual volume of the concrete and the summation of volumes of the components in the mix design for the concrete.

Thus,

$$\varepsilon = 1 - \left[\frac{\text{Actual volume of concrete sample}}{\text{Sum of volumes of the individual components in the concrete mix}}\right] \tag{6}$$

Since the sample is completely dried prior to the water influx experiments, the water volume is neglected for calculating $\varepsilon\cdot\varepsilon = 0.071$ and 0.063 for the normal and cenosphere–concrete, respectively.

If Washburn kinetics is obeyed, a plot of h versus $t^{1/2}$ should be linear. Fig. 6a shows that this relationship is valid at short times, but not past 10 min. The effective pore sizes are 0.6×10^{-9} m for cenosphere–concrete and 2.2×10^{-9} m for normal concrete. Gummerson et al.

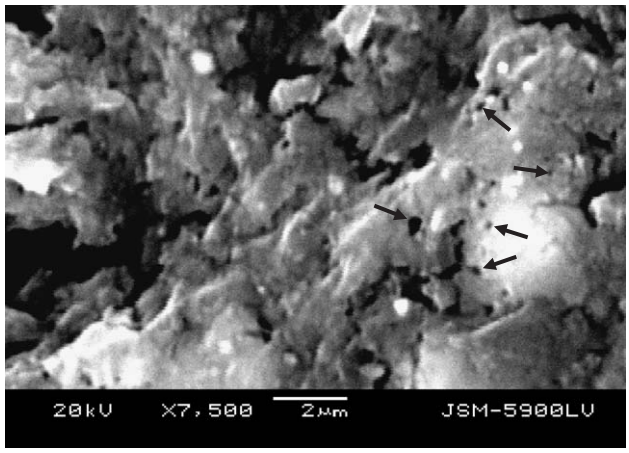

Fig. 7. SEM image of a polished cenosphere–concrete surface showing pores (as shown by arrows). A large deviation between the calculated effective pore size (0.6×10^{-9} m) and the actual size of pores (varying from 2.9×10^{-7} to 5×10^{-7} m) is observed.

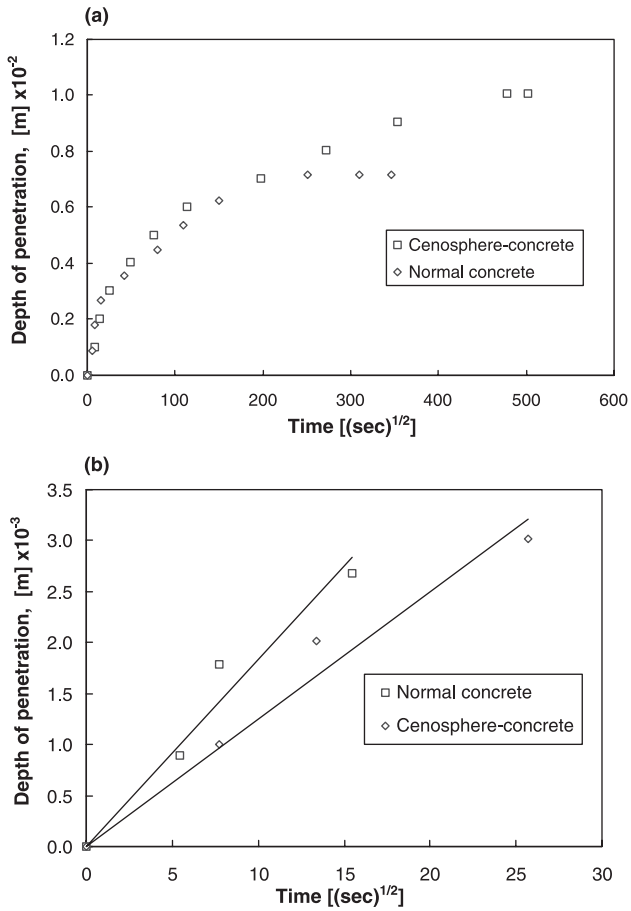

Fig. 6. The variation of h with time and initial weight gain dependence on $t^{1/2}$. The plot indicates the agreement of Washburn kinetics at shorter initial times (5–10 min) for the normal and cenosphere–concrete.

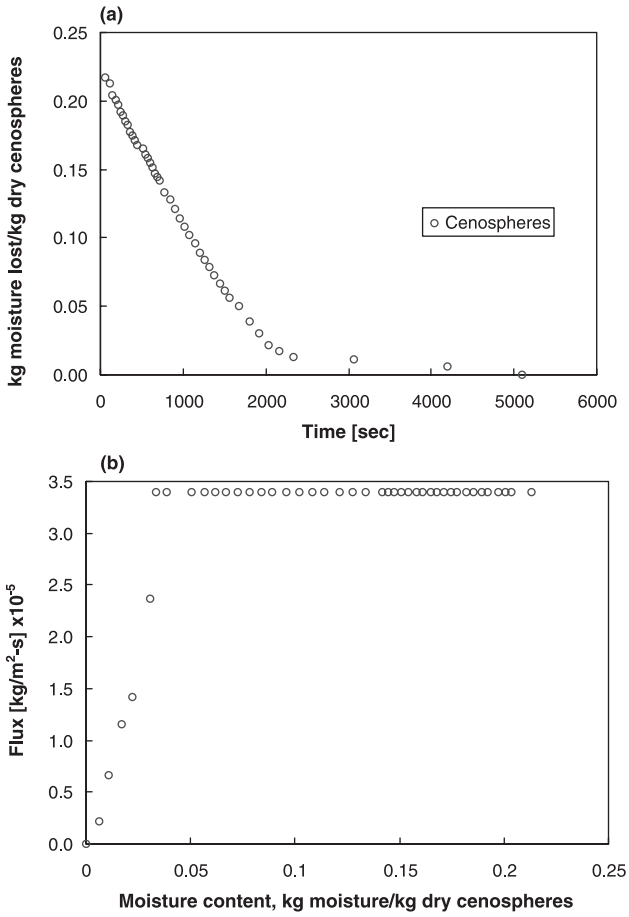

Fig. 8. (a) Moisture content versus time for drying of cenospheres at 23 °C and RH = 45%; (b) drying flux versus moisture content. The data shows classical behavior—a constant-rate drying period followed by a linearly falling rate period.

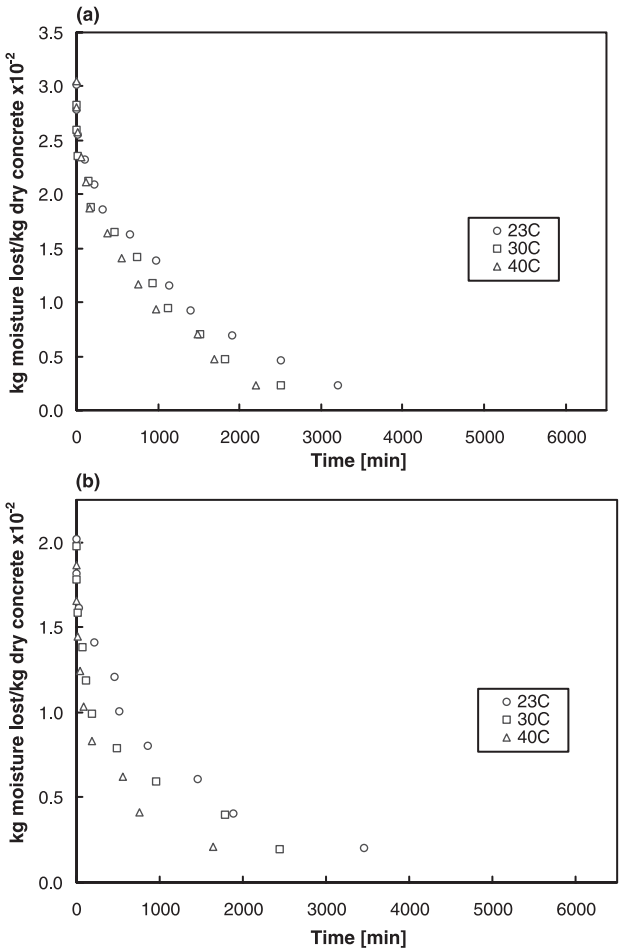

Fig. 9. (a) Moisture content versus time for drying of cenosphere–concrete at 23, 30, and 40 °C and relative humidity of 45%. (b) Moisture content versus time for drying of normal concrete at 23, 30, and 40 °C and relative humidity of 45%.

[12] reported a similar calculation for the effective hydraulic pore radius for brick, which is about 1.5 nm. This low magnitude of the effective pore size indicates that the tortuosity and pore structure strongly impedes the water penetration [12].

An SEM image of a polished cenosphere–concrete is shown in Fig. 7. While the pore size varies widely, it is of the order of 0.5 μm, and is not of the order of 10^{-9} m as predicted from the Washburn equation. This is a clear indication that the pores in the concrete are blocked, leading to the low permeability. The deviation from linearity in the Washburn plots over longer time scales is an artifact of the experimental method, where water fronts approach each other from both right and left. This increases the air pressure within the pockets and slows down water transport.

2.4. Drying of cenospheres and cenosphere–concrete

The cenospheres sample used to study the moisture uptake was allowed to desorb by exposure to dry environment at a relative humidity (45%) at room temperature of 23 °C. Characteristic drying curves for the cenospheres are seen in Fig. 8a and b. As shown in Fig. 8b, a classical drying curve is obtained—a constant rate period followed by a falling rate period until the sample is dry [13]. Experiments done at these conditions can then be used to predict drying behavior in completely different conditions [11] by adjusting for the new mass transfer coefficient and driving force in the new environment.

Drying experiments were performed for saturated cenosphere–concrete and the normal concrete samples at three different temperatures, 23, 30, and 40 °C, by allowing them to dry in air at 45% relative humidity. The data are shown in Fig. 9a and b. Unlike the drying results from the cenospheres alone, the water vapor flux from the cenosphere–concrete as well as the normal concrete shows a highly nonlinear behavior throughout the drying cycle for all temperatures (Fig. 10). Transport of water vapor through the tortuous pores of concrete control the rate of moisture migration to the surface, leading to this observed complex behavior.

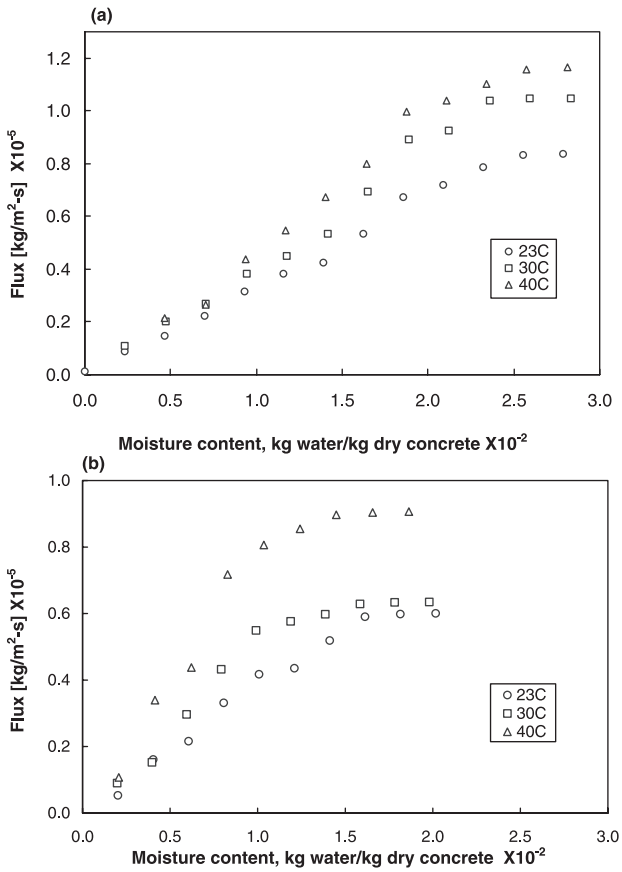

Fig. 10. (a) Drying flux versus moisture content for cenosphere–concrete (b) Drying flux versus moisture content for normal concrete. For each experiment, the temperatures are 23, 30, and 40 °C, and relative humidity is 45%.

3. Conclusions

Detailed experiments monitoring the moisture uptake and loss in cenospheres, sand, and normal as well as cenosphere–concrete samples are undertaken. The moisture uptake by cenospheres is significantly more than the sand, reflecting the porous nature of the cenospheres. Drying experiments for both the cenospheres as well as sand show the classical behavior, where a constant-rate drying period is followed by linear falling rate period. The initial rate of water penetration into concrete shows characteristic $t^{1/2}$ dependence. The effective pore size for water penetration into normal concrete is more than the lightweight cenosphere–concrete, but they are both of the order of 1 nm. These magnitudes indicate that the pores are not connected, leading to a low permeability. The lightweight cenosphere–concrete has higher equilibrium moisture content than the normal concrete. However, normal concrete dries faster than the cenosphere–concrete.

Acknowledgements

Financial support from the Rhode Island Department of Transportation is gratefully acknowledged.

References

[1] E. Berry, R. Hemmings, J. Leidner, Investigation of some new spherical fillers, Plastics Compounding 9 (7) (1986) 12–22.
[2] P. Rohatgi, R. Guo, B. Keshavram, D. Golden, Cast aluminum fly ash composites for engineering applications, Transactions of the American Foundrymen's Society 103 (1995) 575–586.
[3] T. Wandell, Cenospheres: from waste to profits, The American Ceramic Bulletin 75 (6) (1996) 79–81.
[4] F. Blanco, P. Garcia, P. Mateos, J. Ayala, Characteristics and properties of lightweight concrete manufactured with cenospheres, Cement and Concrete Research 30 (11) (2000) 1715–1722.
[5] V. Lilkov, N. Djabarov, G. Bechev, K. Kolev, Properties and hydration products of lightweight and expansive cements: part I. Physical and mechanical properties, Cement and Concrete Research 29 (10) (1999) 1635–1640.
[6] P. Kolay, D. Singh, Physical, chemical, mineralogical, thermal properties of cenospheres from an ash lagoon, Cement and Concrete Research 31 (4) (2001) 539–542.
[7] C. Hall, Barrier performance of concrete: a review of fluid transport theory, Materials and Structures 27 (1994) 291–306.
[8] B. Perez, S. Pantazopolou, M. Thomas, Numerical solution of mass transport equations in concrete structures, Computers and Structures 79 (13) (2001) 1251–1264.
[9] N. Martys, C. Ferraris, Capillary transport in mortars and concrete, Cement and Concrete Research 27 (5) (1997) 747–760.
[10] E. Washburn, Note on a method of determining the distribution of pore sizes in a porous material, Proceedings of the National Academy of Sciences of the United States of America 7 (1921) 115–116.
[11] R.E. Treybal, Mass Transfer Operations, 3rd ed., McGraw-Hill, New York, 1980.
[12] R.J. Gummerson, C. Hall, W.D. Hoff, Water movement in porous building materials: II. Hydraulic suction and sorptivity of brick and other masonry materials, Building and Environment 15 (1980) 101–108.
[13] C. Hall, W.D. Hoff, M.R. Nixon, Water movement in porous building materials—VI, Evaporation and Drying in Brick and Block Materials 19 (1) (1984) 13–20.